ГЕОЛОГИЯ
GEOLOGY

Оригинальная статья / Original paper
https://doi.org/10.30758/0555-2648-2024-70-4-428-443
УДК 55:549:[550.93.552] (99)

Mineral inclusions in the accretion ice above Lake Vostok

German L. Leitchenkov[1,2]✉, Nikolay V. Rodionov[3], Anton V. Antonov[3], Victoria V. Krupskaya[4], Lyudmila Y. Kryuchkova[2]

[1] *All-Russia Research Institute for Geology and Mineral Resources of the World Ocean (VNIIOkeangeologia), St. Petersburg, Russia*

[2] *St. Petersburg State University, St. Petersburg, Russia*

[3] *Russian Geological Institute (VSEGEI), St. Petersburg, Russia*

[4] *Institute of Geology of Ore Deposits, Petrography, Mineralogy and Geochemistry (IGEM) RAS, Moscow, Russia*

✉*leichenkov@vniio.ru*

GLL, 0000-0001-6316-8511; NVR, 0000-0001-5201-1922; VVK, 0000-0002-6127-748X; LYK, 0000-0002-9914-1326

Abstract. The paper is based on additional studies of mineral inclusions in the accretion ice sampled by deep drilling at Vostok Station in central Antarctica. The studies include X-ray microtomography of two mineral inclusions with identification of their mineral composition; analysis of clay minerals in the soft aggregate of the largest inclusion; and geochronological study of zircon grains. X-ray microtomography shows intact morphology of the inclusions in the ice core and their internal texture. The soft aggregate of the largest inclusion is characterized by the dominance of illite, intermediate concentrations of chlorite and small amounts of kaolinite. A notable feature is the absence of mixed-layer minerals typical of Antarctic coastal areas. The most valuable information is derived from new geochronological data and their integration with previous dating data. The detrital zircon U-Pb ages show strong probability peaks between 900 and 1100 Ma, while the detrital monazite ages are clustered between 1250 and 1450 Ma. Both of these age intervals correspond to the Rayner Orogeny.

Keywords: central Antarctica, subglacial Lake Vostok, accretion ice, rock clast, clay minerals, zircon, monazite, geochronology

For citation: Leitchenkov G.L., Rodionov N.V., Antonov A.V., Krupskaya V.V., Kryuchkova L.Y. Mineral inclusions in the accretion ice above Lake Vostok. *Arctic and Antarctic Research*. 2024;70(4):428–443. https://doi.org/10.30758/0555-2648-2024-70-4-428-443

Received 15.04.2024 **Revised 17.05.2024** **Accepted 01.06.2024**

1. Introduction

The ice borehole at Vostok Station passed through the 3769 m-thick East Antarctic ice sheet above Lake Vostok with complete sampling of ice cores, which provided very valuable information on ice properties, palaeoclimate, subglacial environments and other

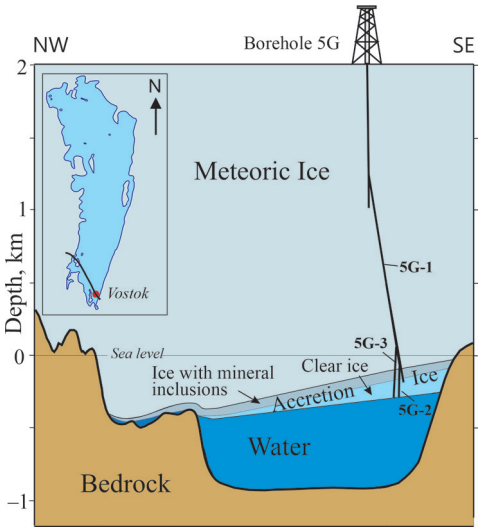

Fig. 1. Ice-water-bedrock section along the ice flow line and across Vostok Station (modified from [3] and borehole 5G with branches 5G-1, 5G-2 and 5G-3; the inset at top left shows the contours of subglacial Lake Vostok (from [9] and the position of the section

Рис. 1. Разрез ледовой толщи, воды и коренного ложа вдоль линии тока льда и через станцию Восток (по [3] с изменениями) и скважину 5Г с ответвлениями 5Г-1, 5Г-2 и 5Г-3; на вставке вверху слева показаны контуры подледникового озера Восток (из [9]) и положение разреза

areas of scientific knowledge [1–3]. Ice core studies show that the ice at this site is divided into 2 main layers according to its origin: the upper one (3537 m thick), formed from atmospheric precipitation, and the lower one (232 m thick), frozen from the water of subglacial Lake Vostok, i. e. accreted from below [4] (Fig. 1). The upper 81 m of accretionary ice (between 3537 and 3618 m), sampled by three borehole branches [5], contains small mineral inclusions, generally less than 1 mm in size, although several intervals contain larger (> 2 mm) inclusions, and the depths of 3606–3608 m are characterized by the presence of the largest inclusions up to 1 cm across [6] (Fig. 2).

Previous studies of 11 inclusions (from depths 3548, 3549, 3550, 3556, 3559, 3561, 3582, 3607, 3608 m) have shown that most of them are represented by soft aggregates consisting mainly of clay matrix, mineral grains ranging in size from 5 to 150 mkm (mainly quartz grains) and rock clasts [3, 7]. Larger inclusions (found mostly in the 3606–3608 m layer) contain rock clasts up to 6–8 mm in diameter. Two inclusions (from 3550 and 3559 m) contain sulfide minerals: pyrite, molybdenite, sphalerite, which may be evidence of hydrothermal activity in Lake Vostok [3].

Lake Vostok is the largest subglacial freshwater reservoir in Antarctica and one of the largest in the world with a water layer up to 1000 m thick [9], but only its southern part provides conditions for water freezing [8] (Fig. 1). The ice sheet drilled at the Vostok station came from the shallow lake area with an island as the site of the present grounded ice [3, 9] (Fig. 1). It is evident that mineral inclusions were trapped in the 81 m thick accreted ice at the time when the ice sheet was flowing over this shallow part of the lake, either from suspension [10] or directly from the lake bottom during ice grounding episodes, which provided grabs of relatively large rock clasts [6] (Fig. 2).

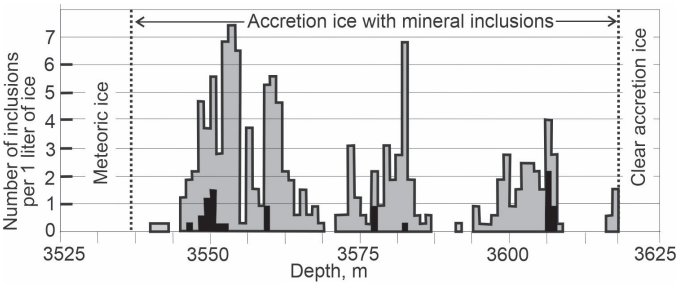

Fig. 2. Calculated concentration of mineral inclusions in the ice cores of accreted ice (borehole 5G-1); the blak shading shows the concentration of relatively large (> 2 mm) inclusions captured from the lake bottom (after [6] with modifications)

Рис. 2. Подсчет концентрации минеральных включений в кернах аккреационного льда (скважина 5Г-1); черной закраской показана концентрация относительно крупных (> 2 мм) включений, захваченных со дна озера (по [6] с изменениями)

Petrographic research, scanning electron microscopy and microanalysis of rock clasts found in the accreted ice (within soft inclusions) allow us to identify these clasts as consolidated, unmetamorphosed quartzose siltstones and sandstones. The bottom sediments trapped in frozen water and incorporated into the ice sheet are thought to be products of ice erosion of the bedrock upstream of southwestern Lake Vostok. The sedimentary nature of this region, known as the Vostok Subglacial Highlands, is also supported by magnetic, gravity and seismic data [3, 11].

All sedimentary rock clasts contained detrital zircon and monazite grains, which were detected by energy dispersive X-ray microanalysis and dated by secondary ion mass spectrometer SHRIMP-II. A total of 31 zircon and 5 monazite grains were dated [3]. Within 7 years since the last publication [3], new data on mineral inclusions in the accreted ice have been obtained. The aim of this paper is to present the results of this additional research. New research includes: 1) X-ray microtomography of two mineral inclusions from a depth of 3606.9 m (branch G-3); 2) examination of rock clasts from a depth of 3606.9 m (branch G-3) with identification of their mineral composition; 3) analysis of clay minerals in the largest soft clast from the 3608 m depth (branch G-1) and, for comparison, in samples from coastal lakes of the Larsemann Hills, Vestfold Oasis (Princess Elizabeth Land) and Banger Hills (western Wilkes Land); 4) geochronological study of 10 zircon grains from the largest (8 mm long) rock clast from the 3608 m depth (branch G-1) and 6 zircon grains from the 4.5 mm long rock clast from a depth of 3607 m (branch G-1).

2. Methods

X-ray computed microtomography was used for the first time to study intact (situated in ice cores) mineral inclusions. The aim of this technology was the recognition of their internal structure and original external morphology. This research was performed at Saint Petersburg State University on a SkyScan 1172 microCT scanner equipped with a cooling stage (Bruker, Belgium).

The rock clasts were studied in the Center of Isotopic Research of the All-Russia Geological Institute (CIR VSEGEI) using a scanning electron microscope (SEM) CamScan MX 2500 equipped with an energy-dispersive X-ray spectrometer Pentafet 10 mm^2 (Oxford Instruments, UK) and SEM TESCAN VEGA3 (TESCAN, Czech Republic) with an energy-dispersive X-ray spectrometer Aztec Ultim 100 mm^2 (OXFORD Instruments, UK).

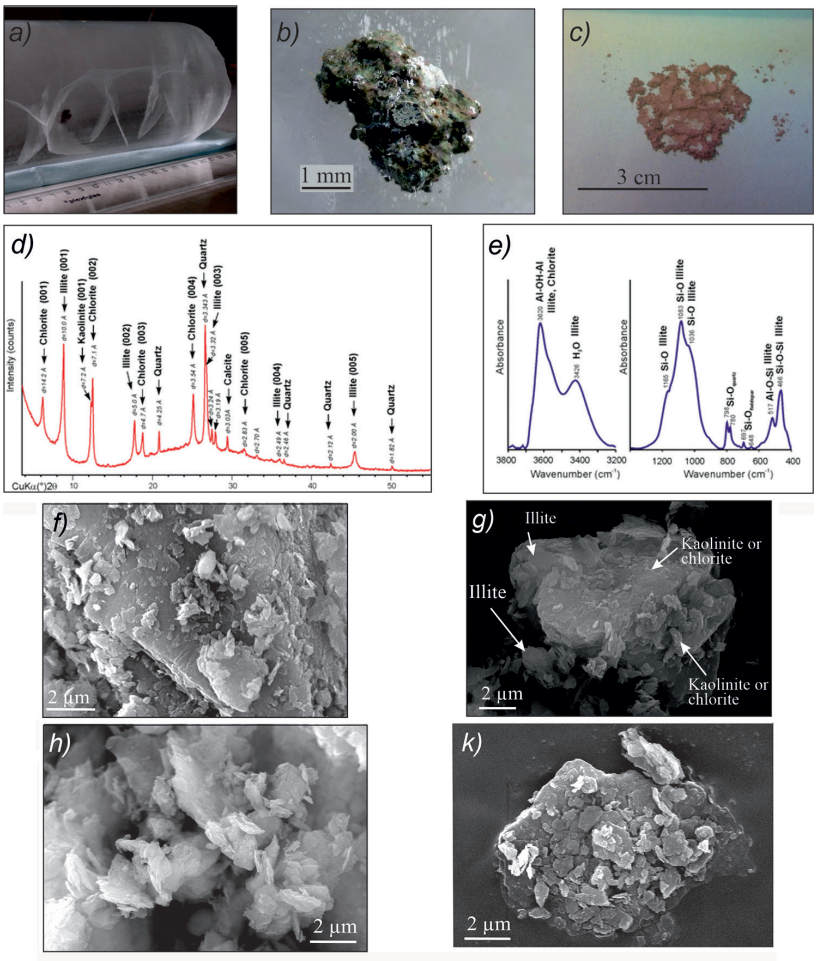

Fig. 3. Study of clay minerals in the largest mineral inclusion from a depth of 3608 m (borehole branch 5G-1).

a — photograph of ice core with the largest mineral inclusion inside; *b* — photograph of the largest intact mineral inclusion (soft aggregate); *c* — dry fine-grained (mostly clayey) residue after drying, which was used for the study of clay minerals; *d* — X-ray diffractogram of the oriented preparation in air-dry state (in brackets are orders of basal reflections for clay minerals); *e* — part of infrared spectra and identification of absorption bands; *f–k* — micrographs obtained with a scanning electron microscope: clay minerals on the surface of the feldspar grain (*f*), aggregate of different clay minerals (*g*), aggregate of illite particles (*h*), aggregate of kaolinite particles (*k*)

Рис. 3. Результаты изучения глинистых минералов в самом крупном минеральном включении с глубины 3608 м (скважина 5Г-1).

a — фотография ледяного керна с крупнейшим минеральным включением внутри; *b* — фотография самого крупного ненарушенного минерального включения (агрегат); *c* — сухой тонкодисперсный (преимущественно глинистый) остаток после высушивания, использованный для изучения глинистых минералов; *d* — рентгеновская дифрактограмма ориентированного препарата в воздушно-сухом состоянии (в скобках указаны порядки базальных отражений для глинистых минералов); *e* — часть ИК-спектров и идентификация полос поглощения; *f–k* — микрофотографии, полученные на сканирующем электронном микроскопе: глинистые минералы на поверхности зерна полевого шпата (*f*), агрегат различных глинистых минералов (*g*), агрегат частиц иллита (*h*), агрегат частиц каолинита (*k*)

The study of clay minerals was carried out in the Institute of Geology of Ore Deposits, Petrography, Mineralogy and Geochemistry and the Geological Institute (Russian Academy of Science) by powder X-Ray diffraction, electronic microscopy and infrared spectrometry using X-Ray diffractometer "Ultima-IV" (RIGAKU, Japan) with a semiconductor detector "DTex/Ultra", SEM LEOSupra 50 VP (Carl Zeiss, Germany) and a FTIR spectrometer "VERTEX 80v" with a DTGS detector and a KBr beamsplitter (Bruker, Germany), respectively.

Infrared spectroscopy (spectra acquisition) was performed in the mid-IR spectral region (4000–400 cm^{-1}) under vacuum pumping conditions with a resolution of 4 cm^{-1}. In order to obtain the most accurate information in the absorption region of the OH-groups, the sample was additionally heated at 150 °C for 20–24 hours. The results obtained were processed using the OPUS 7.0 program. The use of infrared spectroscopy allowed us to correctly apply methods of mathematical modelling of X-ray diffraction patterns from oriented preparations, to calculate the quantitative ratio of clay minerals, and to determine the composition of the amorphous phase. Before the analysis, a fine-grained fraction was extracted from the largest soft aggregate (3608 m; Fig. 3*a*, *b*) and a dry specimen with a weight of approximately 0.5 g was prepared (Fig. 3*c*).

The geochronological study was carried out at CIR VSEGEI using the Sensitive High Mass-Resolution Ion Microprobe (SHRIMP-II, ASI; Australia) following the *in situ* uranium-lead method described by Williams [12]. Zircon grains were preliminarily identified using a SEM CamScan MX 2500 in a cut and polished rock clast mounted in a special preparation for microprobe analysis. Additional zircon grains were found by re-polishing previously cut rock surfaces. Repeat measurements were carried out on two grains to statistically increase the data set.

The intensity of the primary beam of negatively charged molecular oxygen ions was 3 nA with a spot diameter of approximately 20 μm at a depth of up to 2 microns. $^{206}Pb/^{238}U$ ratios in zircon samples were normalised to the Temora-2 zircon standard (416.8 Ma, [13]). Concentrations of lead, uranium and thorium in measured zircon grains were obtained using zircon standard 91500 with a known uranium content of 81.2 ppm [14]. Measured Pb/U ratios of monazite were corrected using reference monazite from the Thompson Mine with a known age of 1766 Ma and U content of 2000 ppm, using the energy filtering technique to reduce the isotopic overlap. The correction for common lead was applied to the value of the measured ^{204}Pb isotope. In some cases where the measured grain size was comparable to or slightly smaller than the analytical spot, the surrounding matrix was analysed to ensure the absence (or insignificant content) of lead, uranium and thorium components. Errors of individual analyses (ratios and ages) are reported at the one sigma level. Raw data were processed using SQUID-1 software [15]; plots of concordia and probability of age distribution were generated using the Isoplot-3 program [15]. The probability density plot consists of ages calculated from the $^{206}Pb/^{238}U$ isotopic ratio for the concordant data and $^{207}Pb/^{206}Pb$ for the few discordant values.

3. Results

3.1. X-Ray microtomography

Two mineral inclusions from a depth of 3606.9 m (branch G-3) were studied using X-ray computed microtomography in ice cubes cut from ice cores (i.e. in intact conditions). The inclusions as a whole have a fanciful shape and consist of relatively large elongated

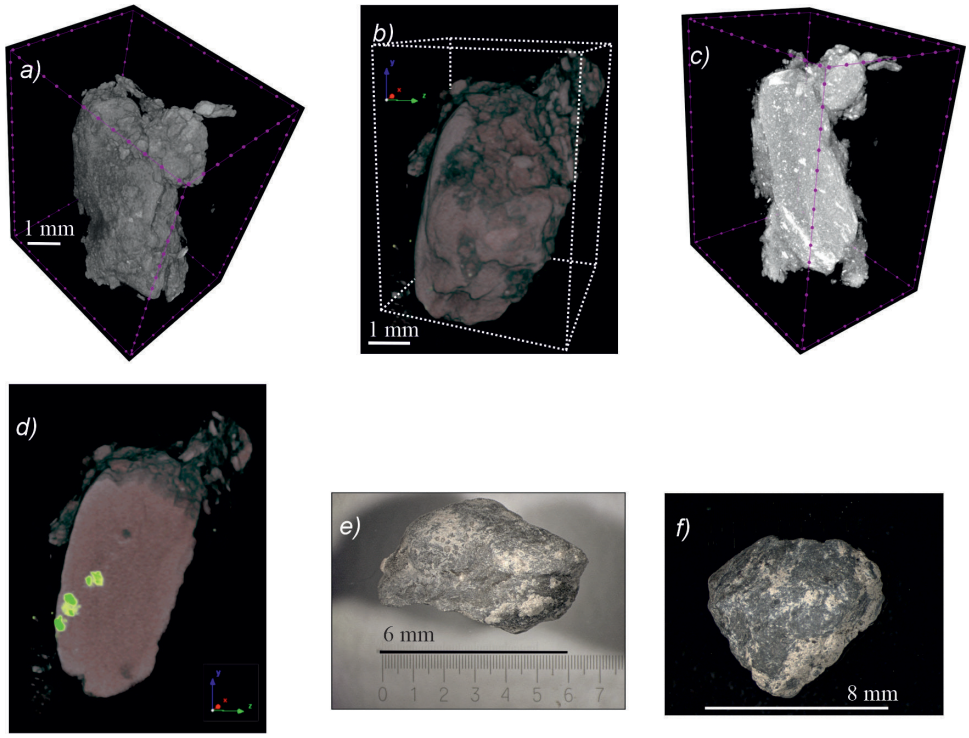

Fig. 4. Images of two inclusions from a depth of 3606.9 m (borehole branch 5G-3).

a, b — Three-dimensional image of mineral inclusions in the ice obtained using of X-ray computed microtomography showing their surface morphology; *c, d* — Three-dimensional images of mineral inclusions in the ice obtained using of X-ray computed microtomography showing sections in the XZ plane (the bright spots are denser mineral grains); *e, f* — photographs of rock clasts after their thawing from the ice and clearing from fine-grained material. The dimensions of 3606.9-3 (1) are 6.3×5.5×2.3 mm, the dimensions of 3606.9-3 (2) are 7.7×5.8×3.5 mm

Рис. 4. Изображения двух включений с глубины 3606,9 м (скважина 5Г-3).

a, b — трехмерное изображение минеральных включений во льду, полученное с помощью рентгеновской компьютерной микротомографии, показывающее морфологию их поверхности; *c, d* — трехмерные изображения минеральных включений во льду, полученные с помощью рентгеновской компьютерной микротомографии, показывающие сечения в плоскости XZ (яркие пятна — более плотные минеральные зерна); *e, f* — фотографии обломков пород после их вытаивания ото льда и очистки от мелкозернистого материала. Размеры 3606,9-3 (1) — 6,3×5,5×2,3 мм, 3606,9-3 (2) — 7,7×5,8×3,5 мм

bodies and numerous small satellites (Fig. 4*a*, *b*). The study shows that the large bodies are rock clasts covered by fine-grained material ranging in thickness from 150 μm to 1.2 mm. Analysis of this material and substance of small satellites using the SEM CamScan MX 2500 revealed a predominance of layered silicates (probably of the hydromica group) and, to a lesser extent, the presence of quartz grains, feldspars and accessory minerals up to 20–30 μm in size. After the ice melted, the cover was almost completely disintegrated exposing the rock clast (Fig. 4*c*).

3.2. Identification of clay minerals

Comprehensive analysis of the fine-grained fraction from the largest soft aggregate (3608 m) showed that the total content of clay minerals is 70–75 % and the other part of the fraction is represented by small grains of quartz, amorphous silica, feldspars and calcite. Infrared spectroscopy showed that the main peaks of the spectra obtained belong to vibrations of Al-OH-Al bonds of illite and chlorite in the region of 3620 cm^{-1}, Si-O bonds of illite in the region of 1165, 1083, 1036 cm^{-1}, and strain vibrations of Al-O-Si (517 cm^{-1}) and Si-O-Si (466 cm^{-1}) of illite.

The clay minerals identified are illite (69 %), chlorite (24 %) and kaolinite (7 %) of terrigenous origin (Figs 3). Illite forms large but thin particles and microaggregates (Fig. 3*h*), while kaolinite is characterized by thicker particles with a pronounced hexagonal shape (Fig. 3*k*). Most of the clay minerals are of terrigenous origin, although authigenic clay minerals have also been detected on the surface of feldspars (Fig. 3*f*). Terrigenous illite is represented by relatively large but thin particles and ultramicroaggregates, while terrigenous kaolinite is characterized by thicker particles with a pronounced hexagonal morphology. In contrast, authigenic clay minerals have much finer particles and a relatively isometric morphology.

Examination of oriented samples in the air-dry state and after saturation with ethylene glycol did not reveal the presence of swelling phases (smectites or mixed-layer formations of the illite-smectite, kaolinite-smectite or chlorite-smectite series). Furthermore, a specific feature of the inclusion in the Vostok ice core is the complete absence of mixed-layer (illite/smectite) clay minerals, which are typical of Antarctic coastal regions (e. g. Shirmacher Oasis, Prince Charles Mountains [16, 17], including those investigated in this study (Larsemann Hills, Vestfold Oasis and Banger Hills).

3.3. Study of rock clasts

Figure 5 shows some of the previously and recently examined rock clasts [2, 3, 7], most of which are quartzose siltstones and sandstones. The largest, 8 mm long, rock clast from the 3608 m depth (Fig. 5, 3608-1) was examined using the SEM CamScan MX 2500S in addition to the petrographic analysis previously performed. It was found that this clast is characterized by very low porosity (1.5 ± 0.5 %) and consists of quartz grains (0.03–0.17 mm across; 69 %), potassium feldspar grains (0.03–0.17 mm across; 18 %) and cement of probable chlorite composition (10 %); the accessory minerals (apatite, garnet, monazite, zircon, iron hydroxides and others (about 1 %). The integral density of the clast, calculated from the distribution of the minerals, their average density and porosity, is estimated to be about 2.6 g/cm^3. Four zircon grains (one 15 μm and three 40 μm in size) were additionally identified in this largest rock clast for for further isotopic analysis.

Two new clasts from a depth of 3606.9 m (branch G-3; Fig. 4*c*; Fig. 5, 3606.9) have been studied by X-ray microtomography and electronic microscope. The first clast (Fig. 5, 3606.9-3(1)) is composed of layered silicates (less than 10 μm in size; about 75–80 %), quartz (30–50 μm in size; 15–20 %), feldspar (about 5 %) and accessory minerals (apatite, rutile, ilmenite, hematite, monazite, zircon; 5–20 μm in size, less than 1 %;). Several well-rounded oval-shaped quartz grains (up to 1 mm in size) are present in the rock mass (Fig. 4*b*). The rock can be defined as silty mudstone. The second clast (Fig. 5, 3606,9-3(2)) is different in its mineral composition and consists mainly of quartz (60–65 %), feldspars (about 30 %), layered silicates (3–5 %) and accessories, but a part of the rock (about 15 % in the section studied) is occupied by a wedge of layered silicates.

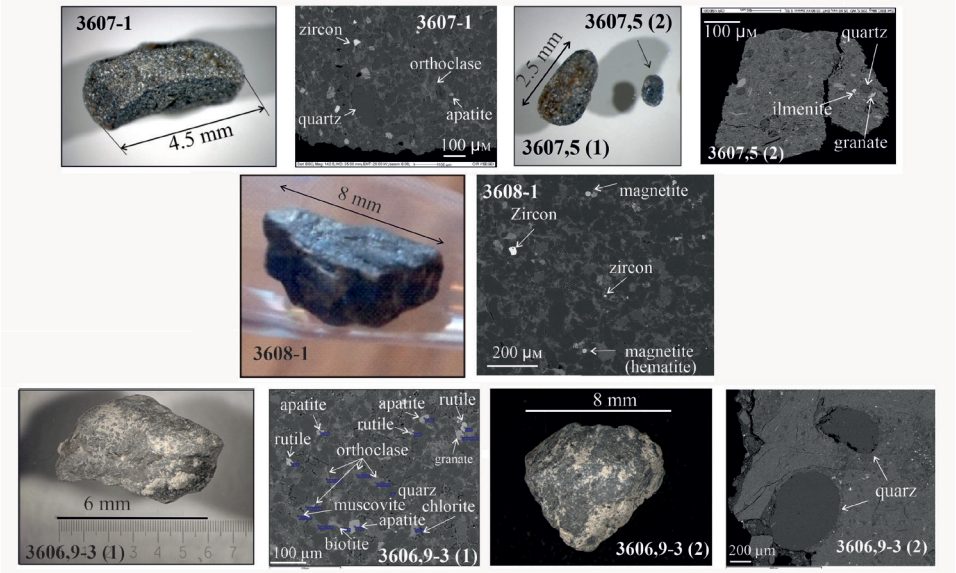

Fig. 5. Photographs of some of the rock clasts studied and backscatter SEM images with identified minerals. Numbers on the images are borehole depths; the number after the hyphen is the hole branch; the number in brackets is the sample number

Рис. 5. Фотографии некоторых изученных обломков пород и изображение их фрагментов в обратно-рассеянных электронах на сканирующем электронном микроскопе

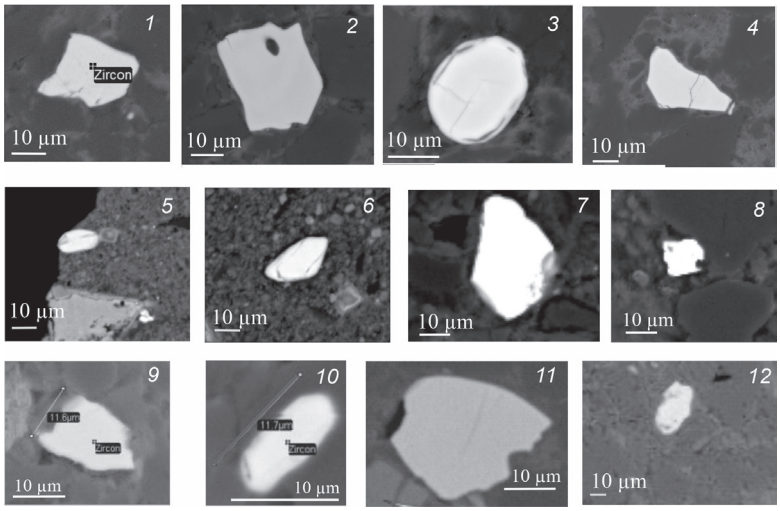

Fig. 6. Backscatter SEM images of zircon and monazite grains showing their type morphology. 1–8: zircon grains (1–7) and monazite grain (8) identified in clast 3608-1 (sandstone); 9–10: zircon grains identified in clast 3606.9-3 (1); 11–12 zircon grains identified in clast 3607

Рис. 6. Изображения зерен циркона и монацита в обратно-рассеянных электронах на сканирующем электронном микроскопе, демонстрирующие их типовую морфологию. 1–8: зерна циркона (1–7) и монацита (8), идентифицированные в обломке 3608-1 (песчаник); 9–10: зерна циркона, идентифицированные в обломке 3606,9-3 (1); зерна циркона, идентифицированные в обломке 3607

3.4. Dating of detrital mineral grains and integration of age data

In addition to the previously dated 31 zircon and 5 monazite grains [3], 10 detrital zircon grains were found in the rock clast from a depth of 3608 m and 6 zircon grains in the rock clast from a depth of 3607 m. Moreover, five age determinations of monazite grains were added from previous studies (not considered in [3]). The size of all the detrital zircon and monazite grains identified ranges from 10 to 50 μm and predominantly from 30 to 40 μm. The zircon grains examined by electron microscopy in sample mounts do not show the primary crystal forms and most of them are rounded in shape, though some of the grains have an angular morphology (Fig. 6).

The zircon U-Pb ages show strong probability peaks at 900, 1000 and 1100 Ma with the latter being the most prominent; the minor but reliable (not less than 5 analyses) peaks are characterized by ages of 900 and 800 million years; and peaks at 760, 1300, 1600, 1750, 2500 Ma (2–3 analyses) can also can be considered as statistically significant (Fig. 7). The monazite age distribution is less reliable due to the relatively small number of analyses. These ages are mainly clustered between 1250 and 1450 Ma and one probability peak falls at 1100 Ma. Isotope ratios of zircon grains suggest that they may be of both magmatic and metamorphic origin.

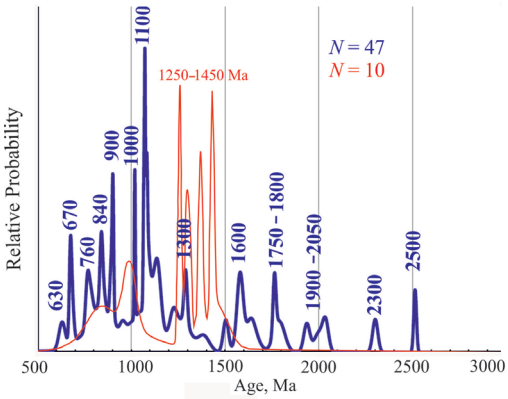

Fig 7. Probability age distribution for zircon ($^{206}Pb/^{238}U$; blue line) and monazite ($^{208}Pb/^{232}Th$; red line) grains. The age peaks (in millions of years) of the zircon grains are shown

Рис. 7. Вероятностное распределение возраста зерен циркона ($^{206}Pb/^{238}U$; синяя линия) и монацита ($^{208}Pb/^{232}Th$; красная линия). Показаны пики возрастов (в миллионах лет) зерен циркона

4. Interpretation and Discussion

4.1. Mineral inclusions

The accretion ice contains several layers of relatively large (>2 mm) mineral inclusions (Fig. 1). The inclusions were extracted from two layers (at depths of 3582 m and 3607–3608 m), and their examination revealed the presence of rock clasts within the soft aggregates (Fig. 5). It can be assumed that all the other large inclusions (or at least most of them) also contain rock clasts.

Royston-Bishop with coauthors [18] suggested that the particles composing the inclusions may have been incorporated into the accretion ice by growing ice crystals and/or by rising frazil ice crystals with upward water circulation. These mechanisms are suitable for fine-grained particles, but relatively large (up to 8 mm long) and heavy (tens to more than hundred milligrams) particles cannot be suspended in the freshwater of the

lake, and so entrapment of rock clasts must have occurred during occasional contacts of the accreting ice with the lake bed at several ice grounding points. The ragged morphology of the lake floor in a shallow bay, which defines different conditions at the bottom of the ice sheet (floating or grounded state), is confirmed by radio-echo sounding [19].

The freezing process was quite slow, with the possible presence of water pockets in the already formed accreted ice, where a suspension of fine-grained material was present. This material was evenly distributed over the surface of the clasts (Fig. 4*a*,*b*).

4.2. Clay minerals

Illite, chlorite and kaolinite, identified in the soft aggregate (inclusion) from a depth of 3608 m are common in Antarctic seas, coastal lakes and outcropped glacial deposits [17, 20]. Illite is the dominant clay mineral and is the product of physical weathering of magmatic and high-grade metamorphic assemblages typical of East Antarctica. However, sedimentary rocks can also be considered as a source of illite, thus, for example, Devonian to Triassic sedimentary succession (Beacon Supergroup) developed in the Transantarctic Mts. is considered to be a source of illite in the Ross Sea Basin [21].

Chlorite is also a widespread mineral, mostly derived from low-grade metamorphic, mafic and sedimentary rocks, and it is not resistant to weathering and long transportation. Kaolinite is a very resistant mineral and is a product of chemical weathering of feldspar and is more characteristic of temperate and tropical latitudes, but can occur in polar regions due to the weathering of older, kaolinite-bearing sediments [20]. The relatively high chlorite content and the presence of kaolinite in the samples studied (Fig. 3) are related to the weathering of the sedimentary rocks underlying the ice, and most likely their cement. The absence of mixed-layer (illite/smectite) clay minerals in the soft aggregates studied suggests that the environmental and weathering conditions in the subglacial environment of central Antarctica and the outcropping regions of the Antarctic margins are significantly different.

4.3. Provenance of detrital zircons

East Antarctica is characterized by a variety of tectonic provinces with ancient metamorphic and magmatic complexes, which are outcropped within coastal regions and well-studied in terms of rock composition, geochronology and geodynamic settings [22, 23] (Fig. 8). Major tectonic subdivisions of East Antarctica are Archean cratons and Proterozoic orogens of different ages (Fig. 8). Crystalline complexes of Archean cratons are unique due to the abundance of tonalite-trondhjemite-granodiorite suites and high- (mostly) to medium-grade metamorphic rocks. The ages of the cratons range between 3.9 to 2.4 Ba, but some parts of them were reworked by younger tectonic processes during the Proterozoic.

The major Proterozoic orogens generally become younger from east to west and are known as the Wilkes, Rayner and Coats-Maud Orogens [23] (Fig. 8). The Wilkes Orogen is thought to underlie the coastal region of Wilkes Land. Exposed rocks include high-grade ortho- and paragneiss and magmatic rocks of varying composition. The dominant age peaks of detrital zircons are ca. 1800–1700 Ma, ca. 1595 Ma and ca. 1380 Ma. Sedimentary protoliths were deposited during the interval 1350–1300 Ma and then intruded during three magmatic events at ca. 1325–1315 Ma, ca. 1250–1210 Ma and ca. 1200–1130 Ma.

The Rayner Orogen is located between Dronning Maud Land and Queen Marie Land, but is best exposed and studied in the Lambert Rift area, where it is composed of high-grade tonalite- and granite orthogneisses, paragneisses and schists, quartzites, metavolcanics, as well as post-kinematic felsic and mafic intrusions. Magmatic and

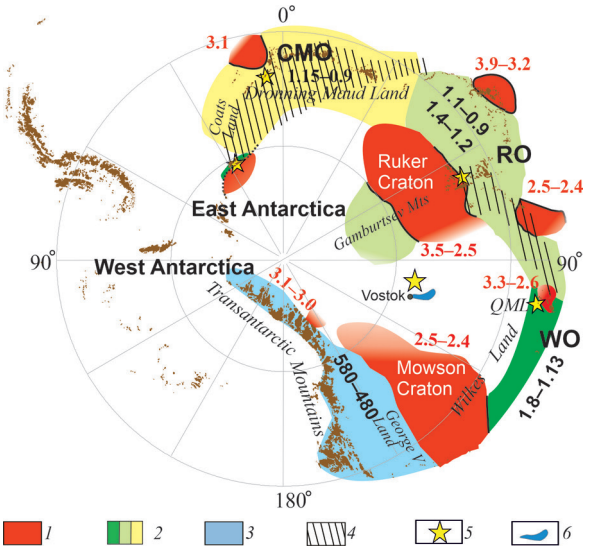

Fig. 8. Major Tectonic provinces of East Antarctica (modified from [23].

1 — Archean Cratons; *2* — Proterozoic Orogens; *3* — Neoproterozoic — Early Paleozoic Ross Orogen; *4* — Early Paleozoic (550–500 Ma) tectono-thermal event (recycling of pre-existing crust); *5* — Late Neoproterozoic — Early Paleozoic sedimentary basins; *6* — Lake Vostok. The red and black numbers (bold font) are the ages of major magmatic and metamorphic rocks of tectonic provinces. Abbreviations: WO — Wilkes Orogen, RO — Rayner Orogen, SMO — Coats-Maud Orogen, QML — Queen Marie Land

Рис. 8. Основные тектонические провинции Восточной Антарктиды (по [23] с изменениями).

1 — архейские кратоны; *2* — протерозойские орогены; *3* — неопротерозойский — раннепалеозойский ороген Росса; *4* — раннепалеозойское (550–500 млн лет) тектоно-термальное событие (переработка ранее существовавшей коры); *5* — поздненеопротерозойские — раннепалеозойские осадочные бассейны; *6* — озеро Восток. Красные и черные цифры (жирный шрифт) — возраст основных магматических и метаморфических пород. Сокращения: WO — ороген Уилкса, RO — Рейнерский ороген, RO — ороген Котса-Мод, QML — Земля Королевы Мэри

metamorphic crystallization events are recorded during two major time intervals: ca. 1400–1250 and 1100–800 Ma [24].

The Coats-Maud Orogen is generally traced in bedrock outcrops from Coast Land to Enderby Land, and its crust was formed during two phases of accretion. The older one is recorded in the western part of the orogen and consists mainly of high-grade complexes dated within 1150–1050 Ma; while the second one is typical of the eastern part of the orogen and is interpreted as the Tonian Oceanic Arc Super Terrane (TOAST), emplaced within 1000-900 Ma interval [26]. Coats-Maud and Rayner orogens experienced Late Neoproterozoic — Early Paleozoic (600–500 Ma) reactivation (orogeny?) involving magmatism of mainly granitoid composition and high- to medium-grade metamorphism [23, 25, 26].

The distribution of tectonic terranes beneath the ice in the Antarctic interior is interpreted from geophysical, mainly magnetic data, which show marked differences in the magnetic field patterns within the cratons and orogens [23]. For instance, magnetic data [26] allow us to identify the tectonic provinces underlying the Gamburtsev Mts. in central Antarctica — the Archean Ruker Craton, which is characterized by an unstructured mosaic field, and the orogenic terrane showing curved linear, extended anomalies similar to those developed within the Rayner Origen (Fig. 8).

Detrital zircon and monazite geochronology is a useful tool for reconstructions of source regions, paleodrainage patterns and paleogeograpy, especially in Antarctica, which is almost entirely covered by ice. The zircon population in the rock clasts studied shows a wide range of ages from Late Neoarchean to Late Neoproterozoic (Fig. 7), reflecting a diversity of Precambrian source terrains. The zircon grains studied are dominated by 900 to 1100 Ma ages, which are typical of the well-studied Rayner Orogen (Fig. 8). This region can therefore be considered as the likely provenance for the majority of the detrital zircon grains found in the rock clasts, though the orogen identified in the southern Gamburtsev Mts. may be a closer and therefore more appropriate source region.

A small population of zircon grains between ca. 1600 and 2050 Ma is thought to be derived from complexes of the Wilkes Orogen bordering the Mawson Craton. Similar zircon U-Pb ages have been obtained from a suite of granitoid clasts collected in glacial catchments draining central East Antarctica from the Transantarctic Mts. to the Gamburtsev Mts. [28]. The oldest (single) peaks of 2300 and 2500 Ma may correspond to the nearby cratonic terrains (Fig. 8).

Of particular interest is the group of well-defined ages between 600 and 800 Ma. The basement outcrops of these ages have not been found in the coastal regions of East Antarctica but may be present in the ice-covered regions of central Antarctica and may record magmatism associated with the crustal extension prior to the break-up of the Rodinia supercontinent. Detrital zircon grains of similar ages have been found in sediments off George V Land, with the proposed provenance located to the south of the Ross Orogeny, whose complexes are outcropped in the Transantarctic Mts [28].

Detrital monazite grains show a predominance of ages between 1450 and 1250 Ma, demonstrating marked differences in age distribution compared to detrital zircon, and minor peaks at ca. 840 and 1000 Ma (Fig. 7). The discrepancies in the age spectra are explained by differences in the physical and petrogenetic characteristics of minerals and because monazite is formed in a broader range of metamorphic conditions, so it can record a wider variety of events than zircon [29]. In our case, the age interval of 1450–1250 Ma corresponds well with the early phase of the Rayner Orogeny, though similar ages are also typical of the Wilkes Orogen (Fig. 8).

Conclusion

Additional studies of mineral inclusions from cores of accretion ice provide new information on their initial (intact) morphology and clay mineralogy, the rock clast they contain, the geochronology of detrital zircon and monazite grains in rock clasts and the provenance of detrital minerals.

1. X-Ray microtomography of ice cores containing rock clasts shows that the clasts are covered with a thin film of fine-grained clayey material. Based on this observation we suggest that the rock clast was captured within the ice grounding zone from the bottom of a shallow bay, located upstream from Vostok Station, and then spent some time in a water pocket with a fine-grained suspension that deposited on the clast surface.

2. Clay minerals, illlite (69 %), chlorite (24 %) and kaolinite (7 %), were identified in fine-grained material of largest mineral inclusion in the accretion ice. The sample studied (as an analogue of lake sediments) is characterized by the absence of mixed-layer (illite/smectite) clay minerals typical of Antarctic coastal regions, which is probably a peculiarity of subglacial weathering in central Antarctica.

3. The detrital zircon U-Pb ages show strong probability peaks at 900, 1000 and 1100 Ma and minor peaks at 760, 800, 900 1300, 1600, 1750 and 2500 Ma, while the detrital monazite ages are mainly clustered between 1250 and 1450 Ma with one probability peak at 1100 Ma. The dominant age group for the detrital zircons between 900 to 1100 Ma corresponds well with the main phase of the Rayner Orogeny manifested in East Antarctica between Dronning Maud Land and Queen Marie Land, though the Gamburtsev Mts with orogenic assemblages of similar ages can be considered as a more probable source region. Detrital monazite grains show a different age distribution compared to detrital zircon, with a predominance of age population between 1450 and 1250 Ma, and these ages are thought to correlate with the early phase of the Rayner Orogeny.

Competing interests. The authors declare no conflict of interest.

Funding. The research was partially fulfilled within the RFBR Project № 15-05-05413 “Geology and environments of subglacial Lake Vostok”.

Acknowledgements. HRXCT studies were done at the Center for X-Ray Diffraction Studies of the Research Park of St. Petersburg State University within the project AAAA-A19-119091190094-6. The authors are grateful to Vladimir Lipenkov (AARI) for providing mineral inclusions from ice cores for the studies. The authors thank the reviewers for carefully reading the manuscript and for helpful suggestions.

Конфликт интересов. У авторов исследования нет конфликта интересов.

Финансирование. Исследование частично выполнено в рамках проекта РФФИ № 15-05-05413 «Природная среда и геологическое строение подледникового озера Восток в центральной Антарктиде».

Благодарности. Исследования на рентгеновском микротомографе проводились в Центре рентгенодифракционных исследований Научного парка СПбГУ в рамках проекта АААА-А19-119091190094-6. Авторы благодарны В.Я. Липенкову (ААНИИ) за предоставление минеральных включений из кернов льда для исследований.

REFERENCE

1. Petit J.R., Jouzel J., Raynaud D., Barkov N.I., Barnola J.M., Basile I., Bender M., Chappellaz J., Davis M., Delague G., Delmotte M., Kotlyakov V.M., Legrand M., Lipenkov V.Ya., Lorius C., Pepin L., Ritz C., Saltzman E., Stievenard M. Climate and atmospheric history of the past 420,000 years from the Vostok ice core, Antarctica. *Nature*. 1999;399(6735):429–436. https://doi.org/10.1038/20859
2. Lipenkov V.Ya., Lukin V.V., Bulat S.A., Vasiliev N.I., Ekaykin A.A., Leitchenkov G.L., Masolov V.N., Popov S.V., Savatyugin L.M., Salamatin A.N., Shibaev Yu.A. Scientific outcomes of subglacial Lake Vostok studies in the IPY. In: Kotlyakov V. (ed.) *Contribution of Russia to International Polar Year 2007/08.* Moscow: Paulsen; 2011. P. 17–47. (In Russ.)
3. Leitchenkov G.L., Antonov A.V., Luneov P.I., Lipenkov V.Y. Geology and environments of subglacial Lake Vostok. *Philosophical Transactions of the Royal Society A.* 2016;374:20140302. https://doi.org/10.1098/rsta.2014.0302
4. Jouzel J., Petit J.R., Souchez R., Barkov N.I., Lipenkov V.Ya., Raynaud D., Stievenard M., Vassiliev N.I., Verbeke V., Vimeux F. More than 200 meters of lake ice above subglacial lake Vostok, Antarctica. *Science.* 1999;286(5447):2138–2141. http://www.jstor.org/stable/2899987
5. Vasilev N.I., Dmitriev A. N., Lipenkov V.Ya. Results of the 5G borehole drilling at Russian Antarctic station “Vostok” and researches of ice cores. *Journal of Mining Institute*. 2016; 2018:161–171.

6. Lipenkov V.Y., Polyakova E.V., Ekaykin A.A. Regularities of congelation ice development in subglacial Lake Vostok. *Ice and Snow.* 2012;4:65–77. (In Russ.). https://doi.org/10.15356/2076-6734-2012-4-65-77
7. Leichenkov G.L., Belyavsky B.V., Antonov A.V., Rodionov N.V., Sergeev S.A. First information about the geology of Central Antarctica based on study of mineral inclusions in ice cores of the Vostok station borehole. *Doklady Earth Sciences.* 2011;440:1207–1211. https://doi/org/10.1134/S1028334X11090054
8. Bell R.E., Studinger M., Tikku A.A., Clarke G.K.C., Gutner M.M., Meertens C. Origin and fate of Lake Vostok water frozen to the base of the East Antarctic ice sheet. *Nature.* 2002;416:307–310. https://doi.org/10.1038/416307a
9. Popov S.V., Masolov V.N., Lukin V.V., Popkov A.M. Russian seismic, radar and seismological studies of subglacial Lake Vostok. *Ice and Snow.* 2012;4:31–38. (In Russ.). https://doi.org/10.15356/2076-6734-2012-4-31-38
10. Souchez R., Petit J-R., Jouzel J., de Angelis M., Tison J.L. Reassessing Lake Vostok's behavior from existing and new ice core data. *Earth and Planetary Science Letters.* 2003;217:163–170. https://doi/org/10.1016/S0012-821X(03)00588-0
11. Studinger M., Bell R., Karner G.D., Tikku A.A., Holt J.W., Morse D.L., Davis L., Richter T.G., Kempf S.D., Peters M.E., Blankenship D.D., Sweeney R.E., Rystrom V.L. Ice cover, landscape setting and geological framework of Lake Vostok, East Antarctica. *Earth and Planetary Science Letters.* 2002;205:195–210. https://doi.org/10.1016/S0012-821X(02)01041-5
12. Williams I.S. U-Th-Pb Geochronology by Ion Microprobe. In: McKibben M.A., Shanks III W.C., Ridley W.I. (eds) *Applications of microanalytical techniques to understanding mineralizing processes.* Littleton: Society of Economic Geologists; 1998. P. 1–35.
13. Black L.P., Kamo S.L., Allen C.M., Davis D.W., Aleinikoff J.N., Valley J.W., Mundil R., Campbell I.H., Korsch R.J., Williams I.S., Foudoulis C. Improved $^{206}Pb/^{238}U$ microprobe geochronology by the monitoring of a trace-element-related matrix effect; SHRIMP, ID-TIMS, ELA-ICP-MS and oxygen isotope documentation for a series of zircon standards. *Chemical Geology*. 2004;205:115–140. https://doi.org/10.1016/j.chemgeo.2004.01.003
14. Wiedenbeck M., Alle P., Corfu F., Griffin W.L., Meier M, Oberli F., von Quadt A., Roddick J.C., Spiegel W. Three natural zircon standards for U-Th-Pb, Lu-Hf, trace element and REE analysis. *Geostandard Newsletter*. 1995;19:1–3.
15. Ludwig K.R. User's Manual for Isoplot 3.75. A geochronological Toolkit for Microsoft Excel. *Berkeley Geochronology Centre Special Publication*. 2012;5:1–71.
16. Ehrmann W.U., Bloemendal J., Hambrey M. J., McKelvey B., Whitehead J. Variations in the composition of the clay fraction of the Cenozoic Pagodroma Group, East Antarctica: implications for determining provenance Werner. *Sedimentary Geology*. 2003;16:131–152. https://doi.org/10.1016/S0037-0738(03)00069-1
17. Srivastava A.K., Khare N., Ingle P.S. Characterization of clay minerals in the sediments of Schirmacher Oasis, East Antarctica: their origin and climatological implications. *Current Science.* 2011;101:363–371.
18. Royston-Bishop G., Priscu J.C., Tranter M., Christner B., Siegert M.J., Lee V. Incorporation of particulates into accreted ice above subglacial Vostok lake, Antarctica. *Annals of Glaciology.* 2005;40:145–150. https://doi.org/ 10.3189/172756405781813555
19. Salamatin A.N., Tsyganova E.A., Popov S.V., Lipenkov V.Y. Ice flow line modeling in ice core data interpretation: Vostok Station (East Antarctica). In: (T. Honda ed.) *Physics of ice core records.* Sapporo, Japan: Hokkaido University Press; 2009. P. 167–194.
20. Ehrmann W.U., Melles M., Kuhn G., Grobe H. Significance of clay mineral assemblages in the Antarctic Ocean. *Marine Geology.* 1992;107(4):249–273.
21. Ehrmann W.U., Setti M., Marinoni L. Clay minerals in Cenozoic sediments off Cape Roberts (McMurdo Sound, Antarctica) reveal palaeoclimatic history. *Palaeogeography, Palaeoclimatology, Palaeoecology*. 2005;229(3):187–211.

22. Cox S. C., Smith Lyttle B., Elkind S., Smith Siddoway C., Morin P., Capponi G. et al. A continent-wide detailed geological map dataset of Antarctica. *Scientific Data.* 2023;10(1):250. https://doi.org/10.1038/s41597-023-02152-9

23. Grikurov G.E., Leychenkov G. *Tectonic Map of Antarctica (Scale 1:10 M) and Explanatory Notes.* Paris: Commission for Geological Map of the World (CGMW); 2023. 1 Sheet, 47 p.

24. Morrissey L.J., Payne J.L., Hand M., Clark C., Taylor R., Kirkland C.L., Kylander-Clark A. Linking the Windmill Islands, east Antarctica and the Albany–Fraser Orogen: insights from U–Pb zircon geochronology and Hf isotopes. *Precambrian Research*. 2017;293:131–149.

25. Mikhalsky E.V., Leitchenkov G.L. (Eds.). *Geological map of Mac.Robertson Land, Princess Elizabeth Land, and Prydz Bay (East Antarctica) in scale 1:1 000 000 (Map Sheet and Explanatory Notes).* St.-Petersburg: VNIIOkeangeologia; 2018. 1 Sheet, 82 p.

26. Jacobs J., Eagles G., Läufer A., Jokat W. New geophysical data from a key region in East Antarctica: Estimates for the spatial extent of the Tonian Oceanic Arc Super Terrane (TOAST). *Gondwana Research.* 2018;9:97–107.

27. Golynsky A.V., Ferraccioli F., Hong J.K., Golynsky D.A., von Frese R.R.B., Young D.A., Blankenship D., Holt J., Ivanov S., Kiselev A.V., Masolov V.N., Eagles G., Gohk K., Jokat W., Damaske D., Finn C., Aitken A., Bell R.E., Armadillo E., Jordan T.A. Greenbaum J.S., Bozzo E., Ganeva G., Forsberg V., Ghidella M., Galindo-Zaldivar J., Bohoyo F., Martos Y.M. Nogi Y., Quartini E., Kim H.R., Roberts J.L. New magnetic anomaly map of the Antarctic. *Geophysical Research Letters*. 2018;45(13):6437–6449. https://doi.org/10.1029/2018GL078153

28. Goodge J.W., Fanning C.M., Fisher C.M., Vervoort J.D. Proterozoic crustal evolution of central East Antarctica: Age and isotopic evidence from glacial igneous clasts, and links with Australia and Laurentia. *Precambrian Research*. 2017;299:151–176. https://doi.org/ 10.1016/j.precamres.2017.07.026

29. Hietpas J., Samson S., Moecher D., Schmitt A.K. Recovering tectonic events from the sedimentary record: Detrital monazite plays in high fidelity. *Geology.* 2010;2:167–170. https://doi.org/ 10.1130/G30265.1

Минеральные включения в аккреационном льду озера Восток

Г.Л. Лейченков[1,2]✉, Н.В. Родионов[3], А.В. Антонов[3], В.В. Крупская[4], Л.Ю. Крючкова[2]

[1] *Всероссийский научно-исследовательский институт геологии и минеральных ресурсов Мирового океана им. академика И.С. Грамберга (ФГБУ «ВНИИОкеангеология»), Санкт-Петербург, Россия*

[2] *Санкт-Петербургский государственный университет (СПбГУ), Санкт-Петербург, Россия*

[3] *Всероссийский научно-исследовательский институт им. А.П. Карпинского (ФГБУ ВСЕГЕИ), Санкт-Петербург, Россия*

[4] *Институт геологии рудных месторождений, петрографии, минералогии и геохимии Российской академии наук (ИГЕМ РАН), Москва, Россия*

✉*leichenkov@vniio.ru*

ГЛЛ, 0000-0001-6316-8511; НВР, 0000-0001-5201-1922; ВВК, 0000-0002-6127-748X; ЛЮК, 0000-0002-9914-13260000

Аннотация. Статья основана на дополнительных исследованиях минеральных включений в кернах аккреационного льда скважины 5Г на станции Восток в Центральной Антарктиде. Исследования включают рентгеновскую микротомографию двух минеральных включений с определением их минерального состава, анализ глинистых минералов в агрегате крупного включения и геохронологическое изучение

зерен циркона. Рентгеновская микротомография показывает неповрежденную морфологию включений в ледяном керне и их внутреннюю текстуру. На основании анализа микрофотографий можно предположить, что обломок породы был захвачен в зоне налегания льда на мелководном участке озера Восток, расположенном выше по течению льда от станции Восток, и затем некоторое время находился в водном кармане с мелкозернистой взвесью, которая оседала на поверхности обломка. Агрегат крупного включения характеризуется преобладанием иллита (69 %), промежуточными концентрациями хлорита (24 %) и относительно небольшим количеством каолинита (7 %). Примечательным является отсутствие смешаннослоистых глинистых минералов, характерных для прибрежных районов Антарктики. Наиболее ценная информация получена из новых геохронологических данных и их интеграции с предыдущими данными датирования. U-Pb возраст детритовых зерен циркона показывает лавные пики на рубежах 900, 1000 и 1100 млн лет, в то время как возраст зерен монацита в основном сгруппирован между 1250 и 1450 млн лет с одним пиком вероятности на рубеже 1100 млн лет. Доминирующая возрастная группа зерен циркона между 900 и 1100 млн лет хорошо согласуется с главной фазой рейнерской орогении, проявленной в Восточной Антарктиде между Землей Королевы Мод и Землей Королевы Мэри, хотя подледные горы Гамбурцева можно рассматривать как более вероятный источник сноса. Зерна монацита, вероятно, отвечают ранней фазе рейнерской орогении.

Ключевые слова: Центральная Антарктида, подледниковое озеро Восток, озерный лед, обломки горных пород, глинистые минералы, циркон, монацит, геохронология

Для цитирования: Leitchenkov G.L., Rodionov N.V., Antonov A.V., Krupskaya V.V., Kryuchkova L.Y. Mineral inclusions in the accretion ice above Lake Vostok. *Проблемы Арктики и Антарктки*. 2024;70(4):428–443. doi.org/10.30758/0555-2648-2024-70-4-428-443

Поступила 15.04.2024 **После переработки 17.05.2024** **Принята 01.06.2024**